Mon. Not. R. Astron. Soc. **000**, 1–?? (2015) Printed 5 January 2016 (MN LATEX style file v2.2)

Thermal mass loss of protoplanetary cores with hydrogen-dominated atmospheres: The influences of ionization and orbital distance

N. V. Erkaev,[1,2] H. Lammer,[3] P. Odert,[3] K. G. Kislyakova,[3]
C. P. Johnstone,[4] M. Güdel,[4] M. L. Khodachenko[3]
[1] *Institute of Computational Modelling SB RAS, 660036, Krasnoyarsk, Russian Federation*
[2] *Siberian Federal University, Krasnoyarsk, Russian Federation*
[3] *Space Research Institute, Austrian Academy of Sciences, Schmiedlstr. 6, A-8042, Graz, Austria*
[4] *Institute for Astronomy, University of Vienna, Türkenschanzstrasse 17, 1180 Vienna, Austria*

arXiv:1601.00452v1 [astro-ph.EP] 4 Jan 2016

Released 2015

ABSTRACT

We investigate the loss rates of the hydrogen atmospheres of terrestrial planets with a range of masses and orbital distances by assuming a 100 times stronger soft X-ray and extreme ultraviolet (XUV) flux. We apply a 1D upper atmosphere radiation absorption and hydrodynamic escape model that takes into account ionization, dissociation and recombination to calculate hydrogen mass loss rates. We study the effect of the ionization, dissociation and recombination on the thermal mass loss rates of hydrogen-dominated super-Earths and compare the results with those obtained by the energy-limited escape formula which is widely used for mass loss evolution studies. Our results indicate that the energy-limited formula can to a great extent over- or underestimate the hydrogen mass loss rates by amounts that depend on the stellar XUV flux and planetary parameters such as mass, size, effective temperature, and XUV absorption radii.

Key words: planets and satellites: atmospheres – planets and satellites: physical evolution – ultraviolet: planetary systems – stars: ultraviolet – hydrodynamics

1 INTRODUCTION

During the early stages of planet formation, protoplanetary cores that are still embedded in the circumstellar disk can accumulate hydrogen-dominated primordial envelopes from the gas disk (e.g., Hayashi et al. 1979; Nakazawa et al. 1985; Wuchterl 1993; Ikoma and Genda 2006; Rafikov 2006; Stökl et al. 2015a; 2015b). The amount of gas captured by the planetary core strongly depends on its mass. Sufficiently massive cores can end up in a runaway accretion regime leading to subsequent formation of gas giants.

Lammer et al. (2014) investigated the origin and loss of captured hydrogen envelopes from protoplanetary cores with masses in the range of 0.1–5$M_\oplus$ orbiting in the habitable zone at 1 AU of a Sun-like G star. In this study, the authors concluded that depending on nebula properties, protoplanetary cores with masses >1.0$M_\oplus$ orbiting within the habitable zone most likely cannot lose their captured hydrogen envelopes. Their results have been recently confirmed by Luger et al. (2015) who studied the transformation of mini-Neptunes into super-Earths in the habitable zones of M dwarfs determined by the loss of atmospheric hydrogen and Johnstone et al. (2015) who investigated the mass loss of hydrogen envelopes around similar cores as assumed by Lammer et al. (2014) along various stellar rotation related activity evolution tracks in the habitable zones of solar-like stars. The results of these studies also indicate that protoplanetary cores with masses $\geqslant$1.5$M_\oplus$ orbiting inside the habitable zone most likely evolve to sub-Neptunes instead of Earth-like planets and keep large fractions of their captured hydrogen envelopes during their whole life times.

In the meantime, the results of these studies are confirmed by observations (Marcy et al. 2014; Rogers 2015). Rogers (2015) analyzed many planets discovered by the Kepler satellite with both radius and mass measurements and concluded that most 'super-Earths' with radii of 1.6$R_\oplus$ have densities that are too low to be composed of silicates and iron alone. The majority of these low density sub-Neptunes are discovered at closer orbital distances than 1 AU. Taking this into account, in this work we study the hydrogen loss rates from captured gas envelopes with core masses of 1$M_\oplus$, 2$M_\oplus$, 3$M_\oplus$ and 5$M_\oplus$ orbiting a moderate rotating young G-star which is 100 times more active in soft X-rays and extreme ultraviolet (XUV) radiation compared to the present

Sun at orbital distances in the range of 0.1 - 1.0 AU. One can expect that at closer orbital distances, due to the larger stellar XUV fluxes, the ionization degrees of gas envelopes will be higher compared to what they would be at 1 AU. Therefore, it is important to study how ionization, dissociation and recombination influence the mass loss rates depending on the orbital location and how the results obtained by the upper atmosphere XUV absorption hydrodynamic escape model differ from those provided by the widely used energy-limited formula (e.g., Lammer et al. 2009; Ehrenreich and Désert 2011; Sanz-Forcada et al. 2011; Leitzinger et al. 2011; Lopez et al. 2012; Lopez and Fortney 2013; Valencia et al. 2013; Kurokawa and Kaltenegger 2013; Luger et al. 2015). In Section 2, we describe the model approach and in Section 3, we discuss the results and compare them with simple estimates carried out by the energy-limited formula.

2 MODEL DESCRIPTION

To study the XUV-heated upper atmosphere structure and thermal escape rates of the hydrogen atoms, we apply an energy absorption and 1-D hydrodynamic upper atmosphere model described in detail in Erkaev et al. (2014; 2015) and Lammer et al. (2013; 2014). The model solves the system of the hydrodynamic equations for mass, momentum, and energy conservation.

In addition to the mechanisms included in our previous models, the simulations in this study also include the effects of ionization, dissociation and recombination. The continuity equations for the number densities of the atomic neutral hydrogen $n_{\rm H}$, atomic hydrogen ions $n_{\rm H^+}$, hydrogen molecules $n_{\rm H_2}$, hydrogen ions $n_{\rm H_2^+}$ can than be written as

$$\frac{\partial\left(n_{\rm H}\right)}{\partial t}+\frac{1}{r^2}\frac{\partial\left(n_{\rm H}vr^2\right)}{\partial r}=-\nu_{\rm H}\phi_{\rm XUV}n_{\rm H}+\alpha_{\rm H}n_e n_{\rm H^+}+ \quad (1)$$

$$2\alpha_{\rm H_2}n_{\rm e}n_{\rm H_2^+}, \quad (2)$$

$$\frac{\partial\left(n_{\rm H^+}\right)}{\partial t}+\frac{1}{r^2}\frac{\partial\left(n_{\rm H^+}vr^2\right)}{\partial r}=\nu_{\rm H}\phi_{\rm XUV}n_{\rm H}-\alpha_{\rm H}n_e n_{\rm H^+}, \quad (3)$$

$$\frac{\partial\left(n_{\rm H_2}\right)}{\partial t}+\frac{1}{r^2}\frac{\partial\left(n_{\rm H_2}vr^2\right)}{\partial r}=-\nu_{\rm H_2}\phi_{\rm XUV}n_{\rm H_2}, \quad (4)$$

$$\frac{\partial\left(n_{\rm H_2^+}\right)}{\partial t}+\frac{1}{r^2}\frac{\partial\left(n_{\rm H_2^+}vr^2\right)}{\partial r}=\nu_{\rm H_2}\phi_{\rm XUV}n_{\rm H_2}-\alpha_{\rm H_2}n_e n_{\rm H_2^+}. \quad (5)$$

The electron density is determined for quasi-neutrality conditions

$$n_{\rm e}=n_{H^+}+n_{H_2^+} \quad (6)$$

and the total hydrogen number density

$$n=n_{\rm H}+n_{\rm H^+}+n_{\rm H_2}+n_{\rm H_2^+}. \quad (7)$$

$\alpha_{\rm H}$ is the recombination rate related to the reaction $H^+ + e \rightarrow H$ of $4\times10^{-12}(300/T)^{0.64}$ cm^3 s^{-1}, $\alpha_{\rm H_2}$ is the dissociation rate of H_2+e $\rightarrow$H + H $2.3\times10^{-8}(300/T)^{0.4}$ cm^3 s^{-1}, $\nu_{\rm H}$ is the hydrogen ionization rate, and ν_{H_2} is the ionization rate of molecular hydrogen (Storey and Hummer 1995; Yelle 2004). The ionization rates are taken from Yelle (2004) but scaled proportionally to the XUV flux that depends on the particular orbit location.

$\phi_{\rm XUV}$ is the function describing the XUV flux absorption in the atmosphere

$$\phi_{\rm XUV}=\frac{1}{4\pi}\int_0^{\pi/2+\arccos(r_{\rm pl}/r)}J_{\rm XUV}(r,\theta)2\pi\sin(\theta)d\theta. \quad (8)$$

Here, $J_{\rm XUV}(r,\theta)$ is the averaged function that describes the variation of the stellar XUV flux as a function of the radial distance due to the atmospheric absorption (Erkaev et al. 2015). The distance r corresponds to the radial distance from the planetary center and $r_{\rm pl}$ is the planetary radius. In the hydrodynamic equations the mass density, ρ, and the pressure, P, can then be written as

$$\rho=m_{\rm H}\left(n_{\rm H}+n_{\rm H^+}\right)+m_{\rm H_2}\left(n_{\rm H_2}+n_{\rm H_2^+}\right), \quad (9)$$

$$P=\left(n_{\rm H}+n_{\rm H^+}+n_{\rm H_2}+n_{H_2^+}+n_{\rm e}\right)kT, \quad (10)$$

where T is the upper atmosphere temperature and k is the Boltzmann constant, and $m_{\rm H}$ and $m_{\rm H_2}$ are the masses of the hydrogen atoms and molecules, respectively. The stellar XUV volume heating rate, $Q_{\rm XUV}$, depends on the stellar XUV flux at the orbital distance of the test planets and on the atmospheric density. $Q_{\rm XUV}$ can then be written as

$$Q_{\rm XUV}=\eta\sigma_{\rm XUV}\left(n_{\rm H}+n_{\rm H_2}\right)\phi_{\rm XUV}, \quad (11)$$

where η is the ratio of the net local heating rate to the rate of the stellar radiative absorption which is typically $\approx 15\%$ in a hydrogen atmosphere (Shematovich et al. 2014). As in Murray-Clay et al. (2009), Erkaev et al. (2013), Lammer et al. (2013) and Lammer et al. 2014) we assume a single wavelength for all photons and use the average XUV photoabsorption cross sections $\sigma_{\rm XUV}$ for hydrogen atoms and molecules of 5×10^{-18} cm^2 and 3×10^{-18} cm^2 for H atoms and H_2 molecules, respectively. The applied values are in agreement with experimental and theoretical data of Bates (1963), Cook and Metzger (1964), and Beynon and Cairns (1965).

One should also note that in pure H_2, H atmospheres, the dominant molecular infra-red (IR) emitting coolant is H_3^+. As shown by Shaikhislamov et al. (2014) and Chadney et al. (2015) this efficient IR-cooling mechanism vanishes or is negligible in hydrogen-dominated upper atmospheres at small orbital distances or high XUV flux values, because due to molecular dissociation preventing the balancing of the stellar heating by IR cooling. Since the assumed XUV flux values related to a young Sun-like star after its arrival at the ZAMS that is applied in our study is high enough, even at 1 AU, that efficient H_3^+ IR cooling plays a negligible role for the studied test planets.

The lower boundary of our simulation domain, $R_0=R_{\rm c}+z_0$, is chosen in a similar way as in Lammer et al. (2014) where $R_{\rm c}$ is the core radius and z_0 the altitude of the gas envelope up to the homopause level that is located at the lower part of the thermosphere. We assume that z_0 remains similar for all the test planets in different orbits. The assumed radii R_0 corresponding to the various core masses have been roughly estimated from envelope mass fractions, $f_{\rm env}$, modeled by Mordasini et al. (2012). We assume $f_{\rm env}$ of ≈ 0.001, ≈ 0.01, ≈ 0.05 and ≈ 0.05 for planetary core masses of $1M_\oplus$, $2M_\oplus$, $3M_\oplus$ and $5M_\oplus$, respectively.

The hydrogen molecule number density at the lower boundary R_0 is assumed to be 5×10^{12} cm^{-3} (e.g., Atreya

1986; Tian et al. 2005; Lammer et al. 2014). For atmospheres that are in long-term radiative equilibrium, the temperature T_0 near the lower boundary of the simulation domain is quite close to the planetary effective temperature $T_{\rm eff}$. The hydrodynamic model is only applicable as long as enough collisions occur, which is the case if Knudsen number < 0.1. We set the upper boundary conditions in the supersonic region assuming the radial derivatives of the density, temperature and velocity vanish.

In the present study, we also compare the mass loss rates obtained by the above described upper atmosphere model with the widely used energy-limited escape formula

$$L_{\rm en} = \frac{\pi \eta R_0 R_{\rm XUV}^2 I_{\rm XUV}}{G M_{\rm pl}}, \quad (12)$$

where $I_{\rm XUV}$ is the stellar XUV flux outside the atmosphere at the orbital location of the planet, $R_{\rm XUV}$ is the effective radius corresponding to the absorption of the stellar XUV flux in the upper atmosphere, and G is Newton's gravitational constant. $R_{\rm XUV}$ depends on the density distribution and can be determined from the following equation (Erkaev et al. 2014; Erkaev et al. 2015)

$$R_{\rm XUV} = R_0^2 \left[1 + 2 \int_{R_0}^{\infty} [1 - J_{\rm XUV}(r, \pi/2)] r dr \right]^{0.5}. \quad (13)$$

As shown by Watson et al. (1981), $R_{\rm XUV}$ can exceed the planetary radius quite substantially, especially for hydrogen-dominated low mass bodies with low gravity fields and high XUV fluxes. For gas giants and other massive and compact planets, $R_{\rm XUV}$ is close to the planetary radius R_0. Therefore, $R_{\rm XUV}$ is often approximated with $R_0 \approx R_{\rm pl}$ in the literature (e.g., Ehrenreich and Désert 2011; Luger et al. 2015)

$$L_{\rm en}^* \approx \frac{\pi \eta R_{pl}^3 I_{\rm XUV}}{G M_{\rm pl}}. \quad (14)$$

To see the difference between both approaches, we compare the results of both assumptions with the hydrodynamic model results. We use the model described above and locate hydrogen-dominated protoplanets with masses of $1 M_\oplus$, $2 M_\oplus$, $3 M_\oplus$ and $5 M_\oplus$ and at orbital locations of 0.1 AU, 0.3 AU, 0.5 AU, 0.7 AU and 1 AU and expose the hydrogen envelopes to XUV flux values scaled corresponding to the orbital locations. We assume the XUV luminosity of the central star is enhanced by a factor of 100 compared to the Sun's present value with a flux at Earth's orbit of ≈ 4.64 erg cm^{-2} s^{-1} (Ribas et al. 2005). However, the enhanced XUV flux assumed in this study corresponds to a moderate rotating solar-like young star but could be more than a factor 3 larger or weaker if the young star is a fast or slow rotator (Tu et al. 2015; Johnstone et al. 2015).

3 RESULTS AND DISCUSSIONS

Table 1 summarizes the thermal hydrogen mass loss rates from the different protoplanets at different orbital locations. It is important to note that the assumed gas envelope masses are negligible compared to the core masses. Depending on the formation scenarios and nebular conditions, similar cores can capture different amount of nebular gas (e.g., Rogers et al. 2011; Mordasini et al. 2012; Stökl et al. 2015). If the captured envelope mass was larger, then R_0 would also move to larger distances. It was shown in Lammer et al. (2014) that in such cases, the mass loss rates would also be higher. As the gas envelope evaporates, R_0 shrinks and as a consequence the mass loss rate also decreases. Because of this effect if one models the mass loss over time the shrinking of R_0 has to be considered (Johnstone et al. 2015). Furthermore, it was shown by Tu et al. (2015) that depending on the initial rotation rate the XUV activity levels of young solar-like stars can evolve very differently during the first Gyr of their life time. We do not study here the mass loss of the test planets for the whole range of possible XUV evolutionary scenarios. The hydrogen mass loss rates shown in Table 1 represent therefore only a phase during the planet's evolution.

Table 1 shows hydrogen mass loss rates calculated using the described hydrodynamic model for all protoplanets at the studied orbital locations neglecting ionization L, neutrals and ions together (L_{ni}) and the losses of only neutral H atoms, $L_{\rm n}$, and H^+ ions, L_i. For comparing the mass loss rates with the energy-limited formula, we show also mass loss rates, $L_{\rm en}$, obtained by this approach, but multiplied with a heating efficiency η of 15 %. Depending on the planetary parameters, the orbital distance, corresponding XUV flux and effective temperature the hydrogen mass loss rates are between the order of $\approx 10^8$ g s^{-1} at 1 AU and $\approx 10^{10}$ g s^{-1} at 0.1 AU. One can also see that $L_{\rm n,i}$ yields negligible differences that are less than a factor 2 for all test planet loss rates between the hydrodynamic upper atmosphere model and the energy-limited formula of eq. (12) at orbital distances of 1 AU. For closer orbits such as 0.5 AU or 0.1 AU, depending on planetary parameters, the differences between the energy-limited formula and the results obtained for $L_{\rm n,i}$ are factors of ≈1.5–3.5 and ≈3.0–9.0, respectively. Therefore, ionization, dissociation and recombination can not be neglected for close orbital distances or highly active young host stars.

Fig. 1 shows the hydrogen mass loss rates for the four planetary masses as a function of orbital distance. One can see that the energy-limited formula underestimates the mass loss rates when one assumes $R_{\rm XUV} \approx R_0 \approx R_{\rm pl}$ (eq. 14) and overestimates the mass loss rates when one uses the more accurate formula of eq. (12). As it is obvious also from Figs 1., eq. (14) tends to underestimate the mass loss rates because of the assumption that the XUV flux is absorbed close to the planetary radius, whereas it is actually absorbed at larger altitudes. For the small planets considered here, $R_{\rm XUV}$ may be located at $2 - 3\,R_0$, much higher than for more massive giant planets (Erkaev et al. 2007; Murray-Clay et al. 2009). Therefore, the application of the energy-limited formula given in eq. (14) is of limited use for low-mass planets.

Moreover, the discrepancy between the mass loss rates calculated with the hydrodynamic code and the energy limited escape formula arises because eq. (12) yields the maximum XUV-driven mass-loss rate that a planet can have, even if multiplied by the heating efficiency η. The numerator represents the integrated XUV heating rate provided to the planet, i.e. the total stellar XUV flux absorbed at $R_{\rm XUV}$ multiplied by the heating efficiency, i.e., the fraction of incident energy converted to heating. Since the denominator represents the potential energy of the planet, eq. (12) assumes that the total absorbed XUV energy is used to lift

Table 1. Hydrogen mass loss rates for protoplanets with masses of $1M_\oplus$ (a), $2M_\oplus$ (b), $3M_\oplus$ (c) and $5M_\oplus$ (d) with assumed hydrogen envelope mass fractions $f_{\rm env}$ as mentioned in the main text and corresponding radii estimated approximately from Mordasini et al. (2012). The hydrogen envelopes are exposed to a stellar XUV flux that is 100 times stronger compared to present solar values at 0.1–1 AU. L is the loss rate calculated with the hydrodynamic model neglecting ionization, dissociation and recombination; $L_{n,i}$ is the total escape rate of hydrogen ions and neutrals if ionization, dissociation and recombination are not neglected; $L_{\rm n}$ and L_i correspond to the losses of neutral H atoms or H^+ ions only. $L_{\rm en}$ and $L^*_{\rm en}$ are the energy limited loss rate cases related to eq. (12) and eq. (14) that have been multiplied by a heating efficiency η of 15 %.

$M_{\rm pl}/M_\oplus$	$R_0/R_\oplus$	$R_{\rm XUV}/R_\oplus$	L [g s^{-1}]	$L_{\rm n,i}$ [g s^{-1}]	$L_{\rm n}$ [g s^{-1}]	$L_{\rm i}$ [g s^{-1}]	$L_{\rm en}$ [g s^{-1}]	$L^*_{\rm en}$ [g s^{-1}]
d=1.0 AU	XUV=100							
$T_{\rm eff}$=250 K	464 erg cm^{-2} s^{-1}							
1	1.15	2.87	2.1×10^{8}	2.1×10^{8}	2.0×10^{8}	8.3×10^{6}	3.3×10^{8}	6.8×10^{7}
2	2.26	5.2	8.5×10^{8}	8.6×10^{8}	8.2×10^{8}	5.0×10^{7}	1.3×10^{9}	2.7×10^{8}
3	2.44	5.12	5.8×10^{8}	5.9×10^{8}	5.6×10^{8}	3.0×10^{7}	9.7×10^{8}	2.2×10^{8}
5	2.71	5.69	6.5×10^{8}	6.7×10^{8}	6.0×10^{8}	6.7×10^{7}	7.2×10^{8}	1.8×10^{8}
d=0.7 AU	XUV=200							
$T_{\rm eff}$=275 K	928 erg cm^{-2} s^{-1}							
1	1.15	2.64	3.6×10^{8}	3.3×10^{8}	3.2×10^{8}	1.3×10^{7}	7.3×10^{8}	1.3×10^{8}
2	2.26	5.1	1.4×10^{9}	1.2×10^{9}	1.1×10^{9}	1.0×10^{8}	2.7×10^{9}	5.2×10^{8}
3	2.44	5.12	8.9×10^{8}	7.7×10^{8}	7.0×10^{8}	6.7×10^{7}	1.9×10^{9}	4.3×10^{8}
5	2.71	4.87	1.1×10^{9}	1.0×10^{9}	9.6×10^{8}	1.0×10^{8}	1.8×10^{9}	3.7×10^{8}
d=0.5 AU	XUV=400							
$T_{\rm eff}$=325 K	1856 erg cm^{-2} s^{-1}							
1	1.15	2.87	5.5×10^{8}	4.8×10^{8}	4.6×10^{8}	2.5×10^{7}	1.7×10^{9}	2.8×10^{8}
2	2.26	5.2	2.0×10^{9}	1.8×10^{9}	1.6×10^{9}	1.8×10^{8}	5.5×10^{9}	1.0×10^{9}
3	2.44	5.12	1.5×10^{9}	1.8×10^{9}	1.3×10^{9}	1.8×10^{8}	3.8×10^{9}	8.3×10^{8}
5	2.71	5.69	2.3×10^{9}	2.0×10^{9}	1.7×10^{9}	3.2×10^{8}	3.2×10^{9}	6.7×10^{8}
d=0.3 AU	XUV=1111							
$T_{\rm eff}$=420 K	5166 erg cm^{-2} s^{-1}							
1	1.15	2.41	2.5×10^{9}	2.8×10^{9}	2.2×10^{9}	6.7×10^{8}	3.3×10^{9}	7.7×10^{8}
2	2.26	4.52	1.1×10^{10}	1.2×10^{10}	7.7×10^{9}	3.8×10^{9}	1.2×10^{10}	2.8×10^{9}
3	2.44	5.36	3.5×10^{9}	3.1×10^{9}	2.5×10^{9}	6.7×10^{8}	1.2×10^{10}	2.5×10^{9}
5	2.71	5.96	4.2×10^{9}	3.5×10^{9}	2.8×10^{8}	6.7×10^{8}	9.7×10^{9}	2.0×10^{9}
d=0.1 AU	XUV=10000							
$T_{\rm eff}$=730 K	46500 erg cm^{-2} s^{-1}							
1	1.15	2.41	1.5×10^{10}	1.8×10^{10}	9.9×10^{9}	8.2×10^{9}	3.0×10^{10}	6.7×10^{9}
2	2.26	3.84	5.7×10^{10}	7.7×10^{10}	3.9×10^{10}	3.9×10^{10}	7.5×10^{10}	2.7×10^{10}
3	2.44	4.63	2.5×10^{10}	3.5×10^{10}	1.5×10^{10}	2.0×10^{10}	8.0×10^{10}	2.2×10^{10}
5	2.71	5.15	1.0×10^{10}	1.7×10^{10}	7.3×10^{9}	1.0×10^{10}	6.5×10^{10}	1.8×10^{10}

the planetary atmosphere out of the planet's gravitational well (Lammer et al. 2015). However, in transonic escape, some fraction of the absorbed energy is also converted to kinetic and thermal energy. In these cases, additional terms increase the denominator and reduce the atmospheric mass loss rate (Sekiya et al. 1980; Johnson et al. 2013; Erkaev et al. 2007; 2015). For certain planetary and stellar parameter combinations, these terms are not negligible leading to a true mass loss rate, as determined with a hydrodynamic model, lower by a factor of a few than those from eq. (12).

Koskinen et al. (2014) therefore suggested to replace η with a mass loss efficiency factor to account for these discrepancies. However, it is difficult to estimate this factor since it depends on planetary and stellar parameters, as illustrated by the variation of this discrepancy for different planets and orbits. On the other hand, for increasing $T_{\rm eff}$ the hydrodynamic mass-loss rates increase, which is also not accounted for in eq. (12) (Johnson et al. 2013; Erkaev et al. 2015). Thus, for very hot planets even eq. (12) could yield lower mass loss rates than does the hydrodynamic model. This is, however, not the case for the planets considered here.

The energy-limited mass loss rates should always be higher than those obtained by the hydrodynamic model. The only exception is if the planetary equilibrium temperature due to the star's entire radiation field (i.e. its bolometric luminosity) is so high that the atmosphere's thermal energy overcomes the gravitational potential of the planet in regions lower than where XUV heating is taking place (Lammer et al. 2015).

One can also see that the inclusion of ionization, dissociation and recombination has only a small effect if one assumes that all neutral atoms and ions can escape from

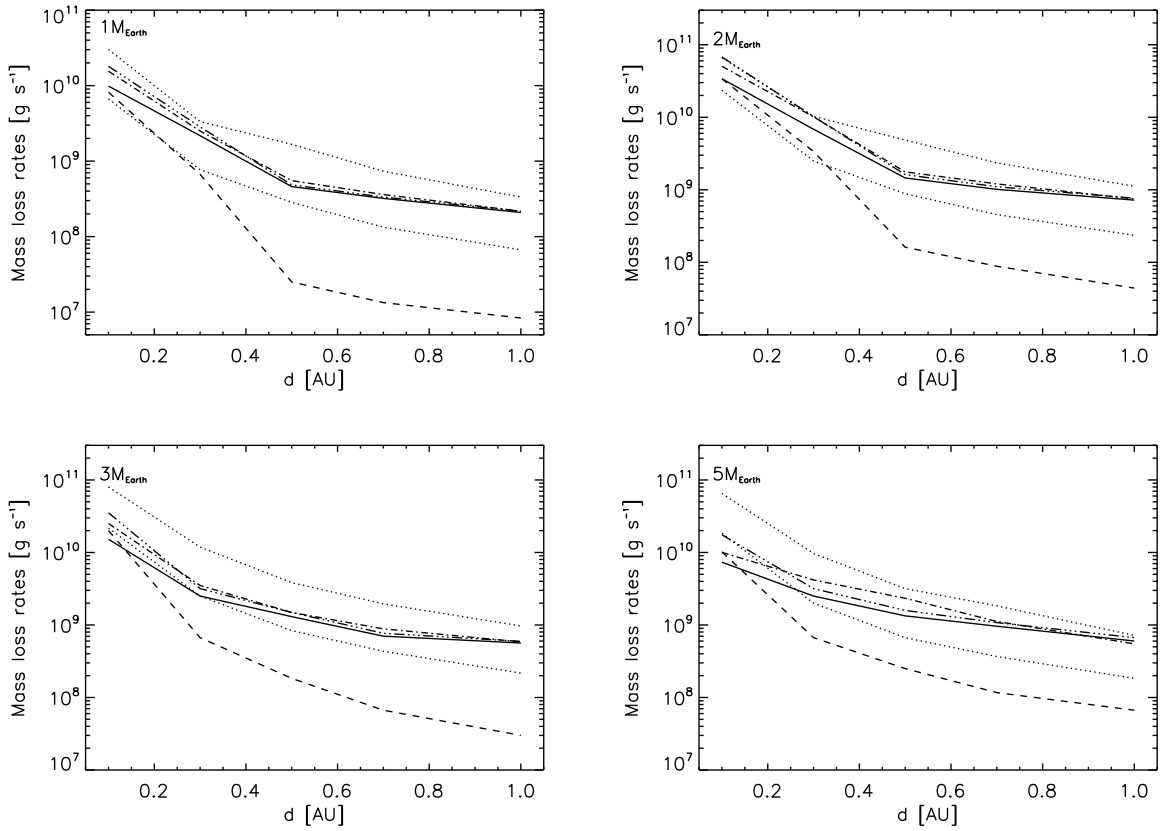

Figure 1. Hydrogen mass loss rates as a function of orbital distance for rocky protoplanetary cores with $1M_\oplus$ (a), $2M_\oplus$ (b), $3M_\oplus$ (c) and $5M_\oplus$ (d) calculated for the stellar XUV flux 100 times higher compared to the present solar value in various orbit locations. The planetary radii related to assumed hydrogen envelope fractions are given in Table 1. Dash-dotted lines correspond to the loss rate L of the hydrodynamic model by neglecting ionization, dissociation and recombination; dash-dotted-dotted-dotted lines correspond to loss rates $L_{\rm n,i}$ if ionization, dissociation and recombination are not neglected; dashed lines correspond to the loss rates $L_{\rm i}$ of ionized hydrogen atoms only; solid lines correspond to the loss rates $L_{\rm n}$ of neutral hydrogen atoms only; the upper dotted lines correspond to the energy-limited loss formula multiplied by a heating efficiency η of 15 %, $L_{\rm en}$ according to eq. (12) and the lower dotted lines correspond to the loss rates $L^*_{\rm en}$ according to eq. (14).

the planets. Only for the more massive planets and extreme high XUV fluxes at close orbital distance (< 0.15 AU) the number density of ions reaches the same value as the neutrals. Different mass loss rates related to neutrals and ions depend strongly on the planetary parameters. Ionization becomes more relevant if the planet is massive and, as a consequence, the upper atmosphere is more compact. Ionization also influences the total mass loss rates because a high degree of ionization reduces the area of the neutral atoms where the stellar XUV flux can be absorbed and heat transferred to neutrals. However, one should note that the above mentioned effect depends strongly on the stellar XUV flux and planetary parameters.

The mass loss rates of the four test planets considered at 0.1 AU are comparable to those of hot Jupiters at 0.045 AU (e.g., Yelle 2004; Koskinen et al. 2013; Shaikhislamov et al. 2014; Khodachenko et al. 2015). As mentioned above, our results represent only a tiny window of possibilities and would be different if the young star was a slow or fast rotator, meaning lower or higher XUV fluxes than assumed in this study. Furthermore, different accumulated nebula gas masses would also change the mass loss rates. If the planets had magnetic moments and resulting magnetospheres, the high degree of ionization at close orbital distances would also reduce the total mass loss rates (Khodachenko et al. 2015). The discovery of many small close-in low density planets at orbital distances < 0.2 AU (Marcy et al. 2014; Rogers 2015) indicates that these objects may have evolved from initially more massive planets to sub-Neptunes and hydrogen-dominated super-Earths, but have never lost their envelopes completely. On the other hand, their host stars could also have been less active stars when they were young.

Fig. 2 shows the mass loss rates of neutrals only, ions only and the sums of neutrals and ions, and hydrodynamic loss rates that consider no ionization, dissociation and recombination, normalized to that corresponding to the energy-limited mass loss rate $L_{\rm en}$ (eq. 12). For very high XUV fluxes, ionization alters the mass loss rates because the increasing number of electrons enhances recombination leading to a large fraction of the energy being lost by cooling radiation (Murray-Clay et al. 2009; Guo 2011). In these studies, for Jupiter-type planets this becomes important for XUV fluxes $> 10^4$ erg cm^{-2} s^{-1}. For considered low mass planets the mass loss rates with ($L_{\rm n,i}$) and with-

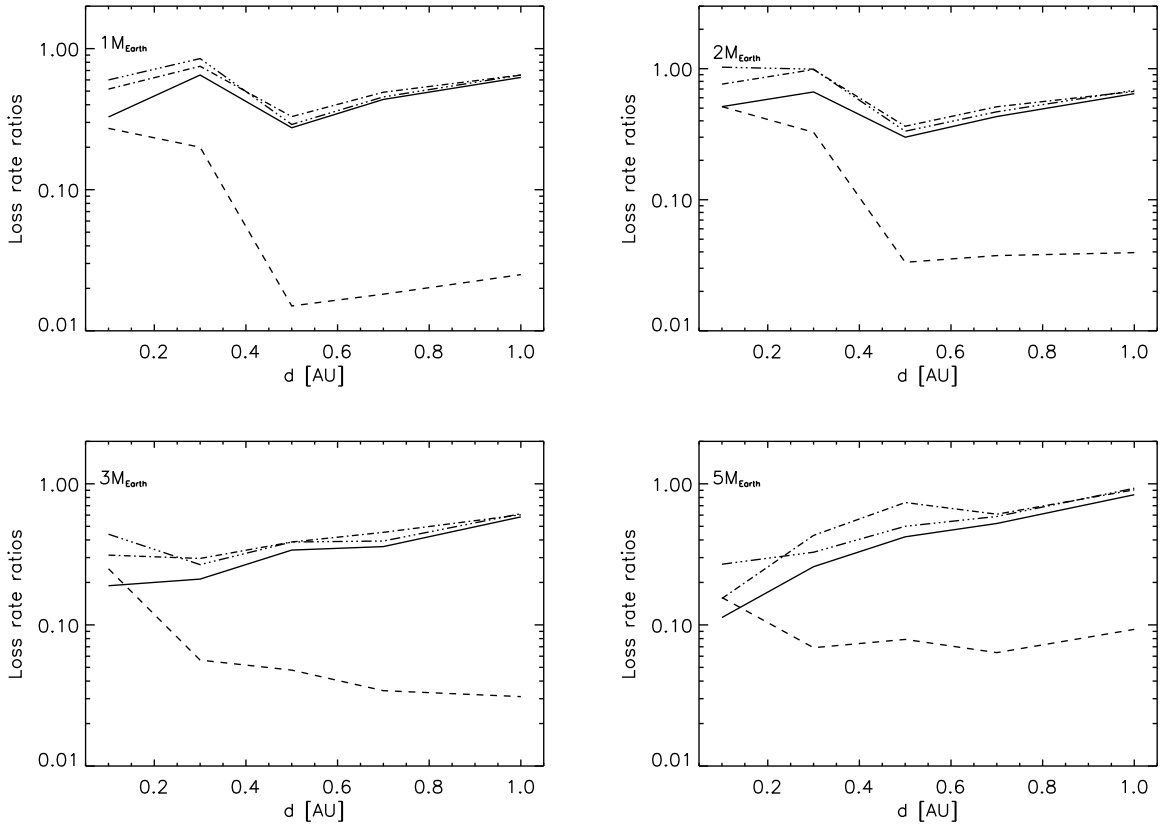

Figure 2. Hydrogen mass loss rates, normalized to that obtained by the energy-limited formula $L_{\rm en}$ of eq. 12. Dash-dotted lines: the loss rates L of the hydrodynamic model by neglecting ionization and recombination; Dash-dotted-dotted lines: loss rates of $L_{\rm n,i}$; dashed lines: ion loss rates $L_{\rm i}$ only; solid lines: neutral atom loss rates $L_{\rm n}$ only.

out ionization (L) are very similar and very small deviations occur only for the closest orbits. This effect would likely become more relevant for even closer orbits or higher stellar XUV emission. In such case, eqs. (12) or (14) are not applicable and approximate estimates for mass loss rates in radiation/recombination-limited regime can be used (Murray-Clay et al. 2009; Owen and Jackson 2012; Luger et al. 2015). One can also see that the rise in ionization occurs for more massive planets with compact upper atmosphere at closer orbital distances, higher effective temperatures and higher XUV fluxes compared to lower mass planets with less compact upper atmospheres.

After having some idea how ionization, dissociation and recombination influence the atmospheric mass loss of hydrogen envelopes around various protoplanetary cores, one can investigate the orbital locations where 'naked' super-Earths or sub-Neptune's which lost their captured nebular gas can be expected. If we use the mass loss rates from Table 1 and estimate roughly how much atmosphere could be lost during the first 100 Myr after the protoatmosphere capture (Lammer et al. 2014) one finds that depending on nebula parameters such as the dust depletion factor $f \approx 0.01$ and assumed relative accretion rates $\frac{\dot{M}_{\rm acc}}{M_{\rm pl}}$ (yr^{-1}) of $\approx 10^{-6}$, cores with masses of $\approx 2M_{\oplus}$ can lose their captured envelopes related to the assumed $f_{\rm env}$, XUV flux most likely within orbital distances that are $\leqslant 0.3$ AU. If the accretion rate is $\approx 10^{-7}$ more massive envelopes can be captured, which would then only be lost at orbital locations $\leqslant 0.1$ AU. A higher dust depletion factor $f \approx 0.1$ would in combination with accretion rates that are $< 10^{-6}$ could remove less massive envelopes from a protoplanetary core with $\approx 2M_{\oplus}$ even at Venus orbit at 0.7 AU. More massive cores if they originate within the nebula lifetime will keep a fraction of their captured hydrogen envelope even at orbital locations of 0.1 AU.

However, a detailed study taking into account the complete parameter space to determine where one can expect that 'naked' super-Earths to be found at orbits that are < 1 AU, has to apply hydrodynamic mass loss calculations that do not neglect ionization, dissociation and recombination and consider all possible stellar XUV evolutionary tracks (Tu et al. 2015), as it was done for the habitable zone by Johnstone et al. (2015). This effort is beyond the scope of the present study but is planned to be carried out in the near future.

4 CONCLUSION

We applied an 1D upper atmosphere radiation absorption and hydrodynamic escape model that includes ionization, dissociation and recombination to hydrogen envelopes captured from protoplanetary nebulae surrounding rocky cores with masses between $1M_{\oplus}$ and $5M_{\oplus}$ at orbital locations of

0.1–1 AU. These different test planets have been exposed to a stellar XUV flux of a young solar-like star emitting 100 times more XUV radiation compared to present Sun. Depending on the assumed planetary parameters, the orbital distance, the corresponding XUV flux and the effective temperature, our model yields hydrogen escape rates of $\approx 10^{32}$ s^{-1} to 10^{34} s^{-1} and corresponding atmospheric mass loss rates of $\approx 10^{8}$ g s^{-1} to 10^{10} g s^{-1} between 1 AU and 0.1 AU, respectively. Our study also shows that the energy-limited formula can overestimate the atmospheric mass loss rates of hydrogen-dominated low mass planets such as 'super-Earths' or sub-Neptunes to a great extent. By assuming that $R_{\rm pl} \approx R_0 \approx R_{\rm XUV}$ the energy-limited formula yields physically incorrect mass loss rates for low mass planets because $R_{\rm XUV}$ can be significantly larger than the planetary radius.

ACKNOWLEDGMENTS

The authors acknowledge the support by the FWF NFN project S11601-N16 'Pathways to Habitability: From Disks to Active Stars, Planets and Life', and the related FWF NFN subprojects, S11604-N16 'Radiation & Wind Evolution from T Tauri Phase to ZAMS and Beyond', and S11607-N16 'Particle/Radiative Interactions with Upper Atmospheres of Planetary Bodies Under Extreme Stellar Conditions'. H. Lammer, P. Odert and N. V. Erkaev acknowledges also support from the FWF project P25256-N27 'Characterizing Stellar and Exoplanetary Environments via Modeling of Lyman-α Transit Observations of Hot Jupiters'. N. V. Erkaev acknowledges support by the RFBR grant No 15-05-00879-a.

REFERENCES

Alibert, Y., 2010, Astrobiology, 10, 19
Atreya, S. K., 1986, Atmospheres and Ionospheres of the Outer Planets and their Satellites. Springer, Heidelberg
Bates, D. R., 1963, Atomic and Molecular Processes, Academic Press, New York.
Beynon, J. D. E., Cairns, R. B., 1965, Proc. Phys. Soc., 86, 1343
Chadney, J. M., Galand, M., Unruh, Y. C., Koskinen, T. T., Sanz-Forcada, J., 2015, Icarus, 250, 357
Cook, G. R., Metzger, P. H., 1964, J. Opt. Soc. Am. 54, 968
Ehrenreich, D., Désert, J.-M., 2011, Astron. Astrophys., 529, A136
Erkaev, N. V., Kulikov, Y. N., Lammer, H., Selsis, F., Langmayr, D., Jaritz, G. F., Biernat, H. K., 2007, Astron. Astrophys., 472, 329
Erkaev, N. V., Lammer, H., Odert, P., Kulikov, Yu. N., Kislyakova, K. G., Khodachenko, M. L., Güdel, M., Hanslmeier, A., Biernat, H., 2013, Astrobiology, 13, 1011
Erkaev, N. V., Lammer, H., Elkins-Tanton, L., Odert, P., Kislyakova, K. G., Kulikov, Yu. N., Leitzinger, M., Güdel, M., 2014, Planet. Space Sci.,98, 106
Erkaev, N. V., Lammer, H., Odert, P., Kulikov, Yu. N., Kislyakova, K. G., 2015, Mont. Notes Roy. Astron. Soc., 448, 1916
Guo, J. H., 2011, Astrophys. J., 733, 98
Hamano, K., Abe, Y., Genda, H., 2013, Nature, 497, 607
Hayashi, C., Nakazawa K., Mizuno H., 1979, Earth Planet. Sci. Lett., 43, 22
Ikoma, M., Genda, H., 2006, ApJ, 648, 696
Johnstone, C. P., Güdel, M., Stökl, A., Lammer, H., Tu, L., Lüftinger, T., Kislyakova, K. G., Erkaev, N. V., Odert, P., Dorfi, E., 2015, ApJ, 815, L12
Johnson, R. E., Volkov, A. N., Erwin, J. T., 2013, Astrophys. J. Lett. 768, L4
Khodachenko, M. L., Shaikhislamov, I. F., Lammer, H., Prokopov, P. A., 2015, Astrophys. J., 813, 50, 18pp
Koskinen, T. T., Yelle, R. V., Harris, M. J., Lavvas, P., 2013, Icarus, 226, 1695
Koskinen, T. T., Lavvas P., Harris M. J., Yelle R. V. 2014, Phil. Trans. R. Soc. A, 372, 20130089
Kurokawa, H., Kaltenegger, L., 2013, Mont. Not. Roy. Astron. Soc., 433, 3239
Lammer, H., et al., 2009, Astron. Astrophys., 506, 399
Lammer, H., Erkaev, N. V., Odert, P., Kislyakova, K. G., Leitzinger, M., 2013, Mont. Notes Roy. Astron. Soc., 430, 1247
Lammer, H., Stökl, A., Erkaev, N. V., Dorfi, E. V., Odert, P., Güdel, M., Kulikov, Yu. N., Kislyakova, K. G., Leitzinger, M., Mont. Not. Roy. Astron. Soc., 439, 3225
Lammer, H., Erkaev, N. V., Fossati, L., Juvan, I., Odert, P., Guenther, E., Kislyakova, K. G., Johnstone, C., Lftinger, T., Güdel, M., 2015, Proc. Natl. Acad. Sci., submitted
Leitzinger, M., et al., 2011, Planet. Space Sci., 59, 1472
Lopez, E. D., Fortney, J. J., 2013, Astrophys. J., 776, 11
Lopez, E. D., Fortney, J. J., Miller, N., 2012, Astrophys. J., 761, 59
Luger, R., Barnes, R., Lopez, E., Fortney, J., Jackson, B., Meadows, V., 2015, Astrobiology, 15, 57
Marcy G W, Weiss L M, Petigura E A, Isaacson H, Howard A W, Buchhave L A., 2014, Proc. Natl. Acad. Sci., 111(35), 12655
Mizuno, H., Nakazawa, K., Hayashi, C., 1978, Prog. Theor. Phys., 60, 699
Mizuno, H., 1980, Prog. Theor. Phys., 64, 544
Montmerle, T., Augereau, J.-C., Chaussidon, M., Gounelle, M., Marty, B., Morbidelli, A., 2006, Earth Moon Planets, 98, 39
Mordasini, C., Alibert, Y., Georgy, C., Dittkrist, K.-M., Henning, T., 2012, Astron. Astrophys. 545, A112
Murray-Clay, R. A., Chiang, E. I., Murray, N. 2009, ApJ, 693, 23
Nakazawa, K., Mizuno, H., Sekiya, M., Hayashi, C., 1985, J. Geomag. Geoelectr., 37, 781
Owen, J. E., Jackson, A. P., 2012, Mont. Not. Roy. Astron. Soc., 425, 2931
Rafikov, R. R., 2006, ApJ, 648, 666
Ribas, I., Guinan, E. F., Güdel, M., Audard, M., 2005, ApJ 622, 680
Rogers, L. A., Bodenheimer, P., Lissauer, J. J., Seager, S., 2011, Astrophys. J., 738, A59
Rogers, L. A., 2015, Astrophys. J., 801, 41
Sanz-Forcada, J., Micela, G., Ribas, I., Pollock, A. M. T., Eiroa, C., Velasco, A., Solano, E., Garćÿa-Álvarez D., 2011, Astron. Astrophys., 532, A6
Sekiya, M., Nakazawa, K., Hayashi, C., 1980, Prog. Theoret. Phys., 64, 1968
Shaikhislamov, I. F. , Khodachenko, M. L., Sasunov, Yu.

L., Lammer,H., Kislyakova, K. G., Erkaev, N. V., 2014, Astrophys. J., 795, 132, 15pp
Shematovich, V. I., Ionov, D. E., Lammer, H., 2014, Astron. Astrophys., 571, A94
Stevenson, D. J., 1982, Planet. Space. Sci., 30, 755
Storey, P. J., Hummer, D. G., 1995, Mon. Not. R. Astron. Soc., 272, 41
Stökl, A., Dorfi, E. A., Lammer, H., 2015a, A&A, 576, A87
Stökl, A., Dorfi, E. A., Lammer, H., 2015b, A&A, submitted
Tian, F., Toon, O. B., Pavlov, A. A., De Sterck, H., 2005, ApJ, 621, 1049
Tu, L., Johnstone, C. P., Güdel, M., Lammer, H., 2015, Astron. Astrophys., 577, L3
Watson, A. J., Donahue, T. M., Walker, J. C. G., 1981, Icarus 48, 150
Wuchterl, G., 1993, Icarus, 106, 323
Yelle, R.V., 2004, Icarus, 170, 167